

Strut-and-tie model design provisions

**Robin G. Tuchscherer,
David B. Birrcher,
and Oguzhan Bayrak**

In this paper, the strut-and-tie design provisions recommended by *Building Code Requirements for Structural Concrete (ACI 318-08)* and *Commentary (ACI 318R-08)*,¹ the American Association of State Highway Transportation Officials' *AASHTO LRFD Bridge Design Specifications, 4th Edition—2008 Interim Revisions*,^{2,3} and the *fib* (International Federation for Structural Concrete) *Structural Concrete, Textbook on Behaviour, Design, and Performance*⁴ are evaluated with a database of deep-beam test results.

Based on an analysis of these results, the provisions in the AASHTO LRFD specifications and ACI 318-08 were found to be inefficient and overly conservative. A new design procedure was developed to improve the efficiency and accuracy of the strut-and-tie design provisions.

The new design procedure is calibrated using only those test specimens that are most representative of actual structures in the field, in terms of both their size and reinforcement details. The new design procedure is largely based on the design provisions recommended in *fib* structural concrete. Minor improvements to the *fib* structural concrete provisions are proposed in order to maintain consistency with ACI 318-08 and AASHTO LRFD specifications. When establishing the design procedure, consideration was given to simplicity, coordination with experimental data and theory, and coordination with standard design provisions.

Background

Typically, reinforced concrete members are designed to resist shear and flexural forces based on the assumption that strains vary linearly at a section. Referred to as the Bernoulli hypothesis or beam theory, the mechanical behavior of a beam is commonly determined by assuming that plane sections remain plane. The region of a structure where the Bernoulli hypothesis is valid is referred to as a B region. In B regions, the internal state of stress can be derived from the equilibrium of forces at a discrete cross section. Therefore, the design of these regions is often referred to as sectional design.

A deep-beam design must be treated differently from a sectional design (or slender beam design) because the as-

Editor's quick points

- This research project develops simple and safe design guidelines for deep beams.
- A database of 868 deep-beam tests was assembled from previous research, and 37 beams were fabricated and tested.
- A new and simple strut-and-tie modeling procedure was proposed for the strength design of deep-beam regions.

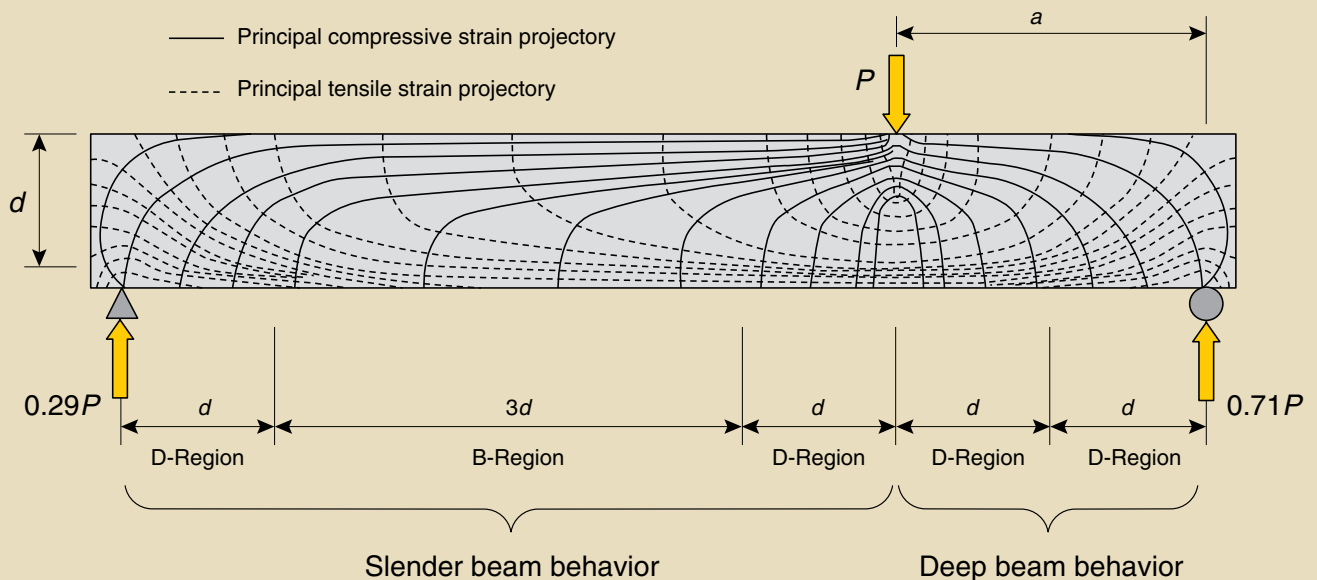


Figure 1. This figure shows the strain distribution in the deep and slender portion of a beam. Note: a = shear span; B region = region of a structure where the Bernoulli hypothesis is valid; d = distance from extreme compression fiber to centroid of longitudinal tension reinforcement; D region = region of discontinuity caused by abrupt changes in geometry or loading; P = axial load.

assumptions used to derive the sectional theory are no longer valid. In practice, engineers commonly encounter deep beams when designing transfer girders, pile-supported foundations, shear walls, or corbels. In principle, a deep beam is a member with a relatively small shear span-to-depth ratio a/d , such that nonlinear shearing strains dominate the behavior. Nonlinear strain distributions are caused by abrupt changes in geometry or loading. These regions of discontinuity are referred to as D regions. An elastic stress analysis suggests that the localized effect of a concentrated load or geometric discontinuity will attenuate about one member depth d away from a discontinuity (St. Venant's principle). For this reason, D regions are assumed to extend one member depth from the load or discontinuity. A deep beam often comprises both a concentrated load and support discontinuity. Therefore, nonlinear behavior can be expected if the load point is located less than twice the member depth $2d$ from the support. MacGregor⁵ defines a deep beam as follows: "a beam in which a significant amount of load is carried to the supports by a compression thrust joining the load and the reaction. This occurs if a concentrated load acts closer than about $2d$ to the support, or for uniformly loaded beams with a span-to-depth ratio, l_n/d , less than about 4 to 5."

Figure 1 illustrates a B region and a D region for an asymmetrically loaded, simply supported beam. The left side of the beam contains a B region, and stresses can be determined according to sectional methods. The right side contains a concentrated load located twice the member depth $2d$ from the support. Here, shear strains dominate the behavior, and beam theory cannot be used to determine the internal state of stress.

ACI 318-08 and AASHTO LRFD specifications adopted strut-and-tie modeling in 2002 and 1994, respectively, for the design of deep beams or other regions of discontinuity. A strut-and-tie model (STM) idealizes the complex flow of stresses in a structural member as axial elements in a truss member. Concrete struts resist the compressive stress fields, and reinforcing steel ties resist the tensile stress fields. Struts and ties intersect at regions called nodes. Nodes are named based on the nature of the elements that frame into them. The notation used to denote nodal zones is as follows:

- CCC: nodal zone bounded by three or more struts
- CCT: nodal zone bounded by two or more struts and a tie
- CTT: nodal zone bounded by a strut and ties in two or more directions

If more than three forces intersect at a node, it is often necessary to resolve some of the forces to end up with three resulting forces. For a simply supported beam, a CCC node generally occurs under the applied load and a CCT node occurs at the support. Struts, ties, and nodes are the three elements that comprise an STM, and they must be proportioned to resist the applied forces. According to the lower-bound theory of plasticity, the capacity of an STM is always less than the actual capacity of the structure if the following requirements are met:

- the truss is in equilibrium

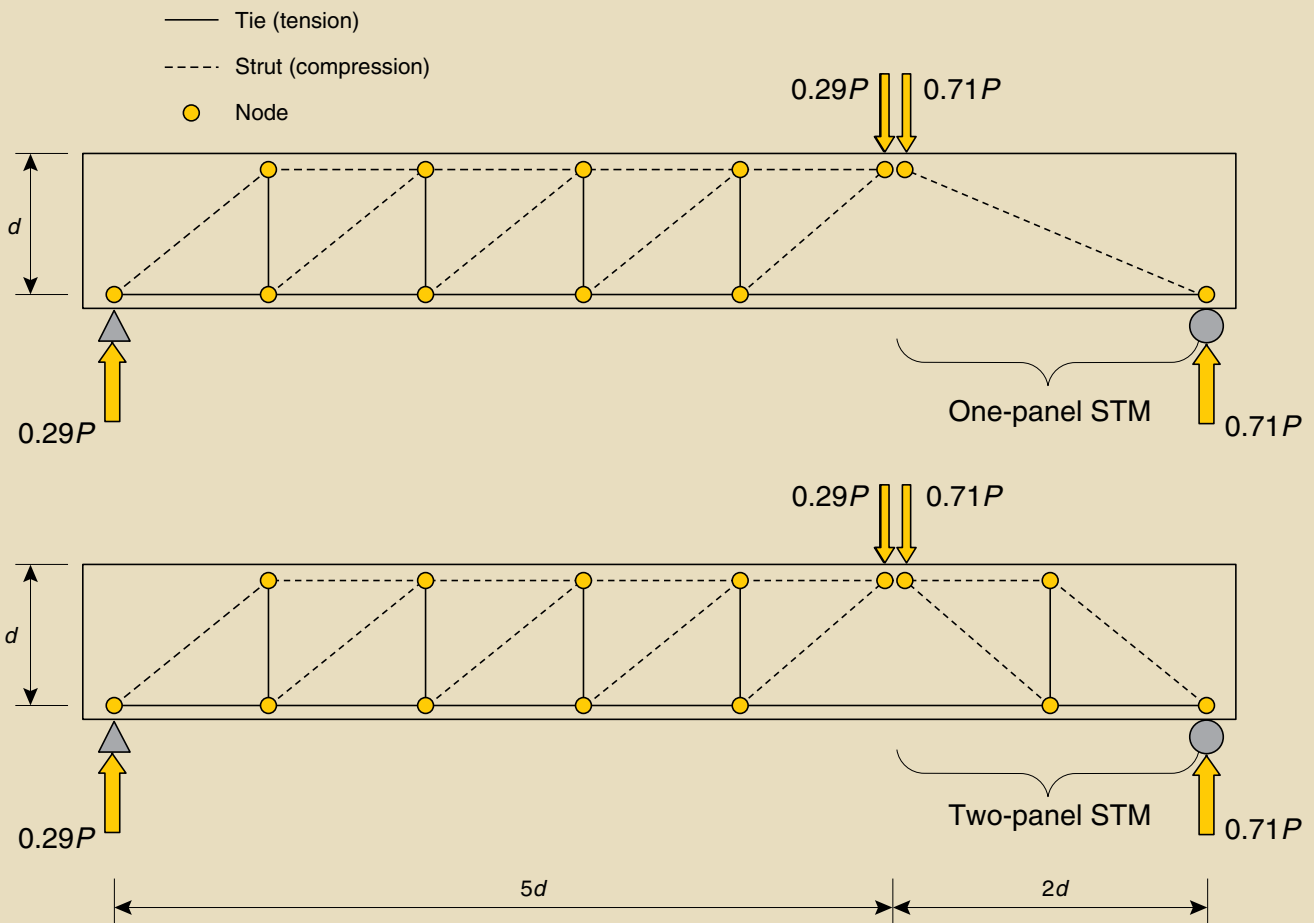


Figure 2. This figure shows both a one-panel and a two-panel strut-and-tie model that can be used to represent a deep-beam region. Note: d = distance from extreme compression fiber to centroid of longitudinal tension reinforcement; P = axial load; STM = strut-and-tie model.

- sufficient deformation capacity exists to distribute forces according to the assumed truss model
- the stresses applied to the elements do not exceed their yield or plastic flow capacity

If the yield capacity of an element is exceeded, the failure modes of a deep beam are the crushing of concrete in a strut or at the face of a node, yielding of a tie, or anchorage failure of a tie.

When designing a deep-beam region using an STM, the first step is to determine the configuration of the truss model and the resulting forces in the critical elements.

Figure 2 provides two STMs for the beam depicted in Fig. 1. In this paper, the first model is referred to as a single- or one-panel model; the second is called a multiple- or two-panel model.

Either of the two models in Fig. 2 is acceptable if equilibrium and yield conditions are satisfied. The choice of the model is left to the discretion of the designer. However, if the orientation of the truss model varies significantly from the actual stress field, then the structure must undergo sub-

stantial deformation in order to develop the poorly assumed model. Thus, it is good practice for the STM to agree with the dominant mechanism of force transfer in the structure.

Past researchers^{6,7} agree that a direct strut (one-panel model) is the predominant load-carrying mechanism for structures with a/d less than 2.5 to 2. Also, experimental observations of this research⁸ indicated that a direct strut was the primary load transfer mechanism for specimens with an a/d of 1.85. Furthermore, the ACI 318-08 provisions allow a designer to use a single-panel strut when the a/d ratio is less than or equal to 2.1. (This is accomplished indirectly by limiting the strut angle to 25 deg as $\cot 25 = 2.1$.) Accordingly, based on experimental observations, past research, and current design provisions, the beams in this study were evaluated using a single-panel truss model.

Proportioning a strut-and-tie model

After the selection of an STM, defining the geometry of the nodal regions is required to calculate stresses on each nodal face. These stresses are then compared with the allowable design stresses. Generally, there are two techniques for

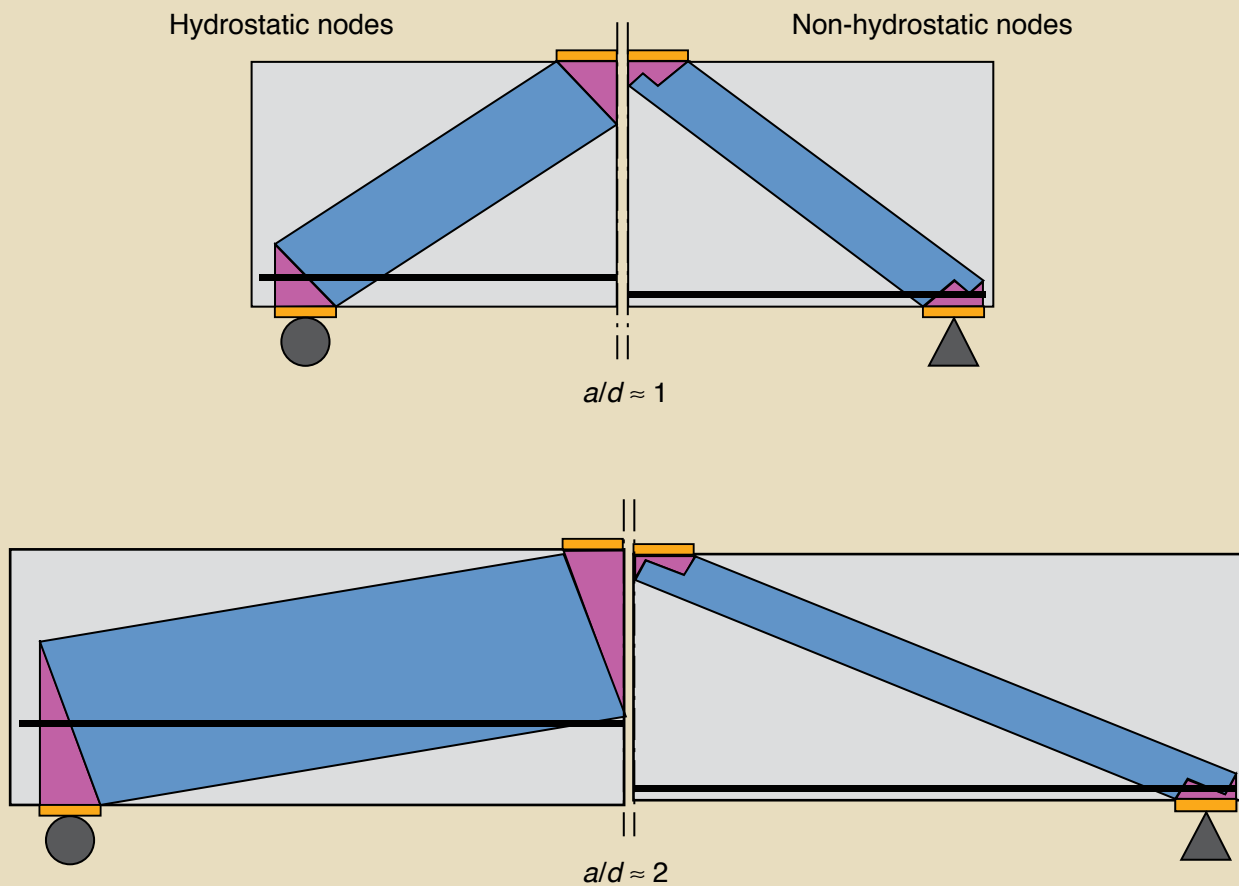


Figure 3. This figure illustrates the influence that a hydrostatic and nonhydrostatic node has on strut proportions. Note: a/d = shear span-to-depth ratio.

proportioning nodes that have been established by previous researchers and code committees. The use of each technique results in either hydrostatic or nonhydrostatic nodes. In both cases, nodal geometry is an idealization of regions in the STM where struts and ties are equilibrated. However, the resulting capacity of a truss model can be different depending on the type of node. **Figure 3** illustrates the influence that each of these node types has on an STM.

When the a/d of a deep-beam region increases, hydrostatic nodes can result in unrealistically large struts (Fig. 3). Alternatively, strut widths resulting from nonhydrostatic nodal regions remain approximately constant as a/d increases.

Principal stresses are equal on all sides of a hydrostatic node. Therefore, the ratio of each nodal face is directly proportional to the force being applied to that face. However, the nodal dimensions are often inconsistent with other beam details, such as the location of the reinforcement and depth of the flexural-compression zone (Fig. 3). Alternatively, the stress applied to each face of a nonhydrostatic node is different because the size is based on these beam details. There is no requirement for equal stresses on all faces of a node. In fact, the techniques used to propor-

tion nonhydrostatic nodal regions have been well established by previous researchers and code provisions. These proportioning techniques are included in the current ACI 318-08, *fib* structural concrete, and AASHTO LRFD specifications. Therefore, in order to maintain consistency with current design practice and code provisions, it is proposed that nonhydrostatic nodal regions be used to determine the critical stresses in a deep-beam shear region.

The use of a consistent truss model is an essential requirement when evaluating code provisions. The critical nodal stresses are entirely dependent on the configuration of the model and geometry of the nodal regions. In this study, a single-panel STM was used to analyze deep-beam test results (**Fig. 4**). Nonhydrostatic nodes were proportioned according to the techniques in **Fig. 5**.

The length of the bearing plate l_b and portion of the load that is transferred to the near support is used to determine the area of the bearing face of a CCC node. Typically, the depth of the back face of a CCC node h_s is taken as the depth of the equivalent compressive stress block obtained from a conventional flexural analysis. For a rectangular beam, Eq. (1) determines h_s .

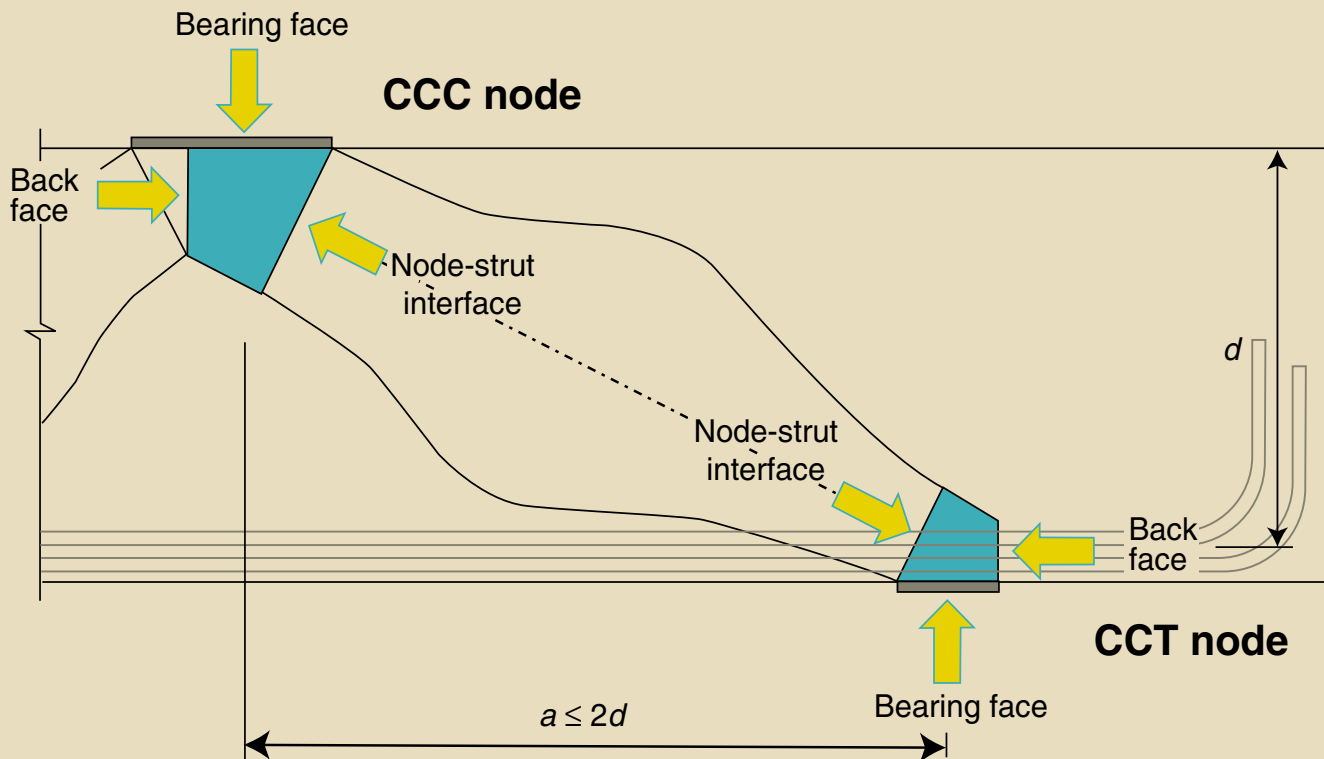


Figure 4. This figure shows a single-panel strut-and-tie model with nonhydrostatic nodal regions. Note: a = shear span; CCC = node framed by three or more intersecting struts; CCT = node framed by two or more intersecting struts and a tie; d = distance from extreme compression fiber to centroid of longitudinal tension reinforcement.

$$h_s = \beta_1 c = \frac{(A_s f_s - A'_s f'_s)}{0.85 b_w f'_c} \quad \text{Eq. (1)}$$

where

β_1 = factor for proportioning the depth of the equivalent stress block in the flexural compression region

c = distance from extreme compression fiber to neutral axis

A_s = area of tension reinforcement

A'_s = area of compression reinforcement

f'_c = specified compressive strength of concrete

b_w = web width

f'_s = stress in compression reinforcement

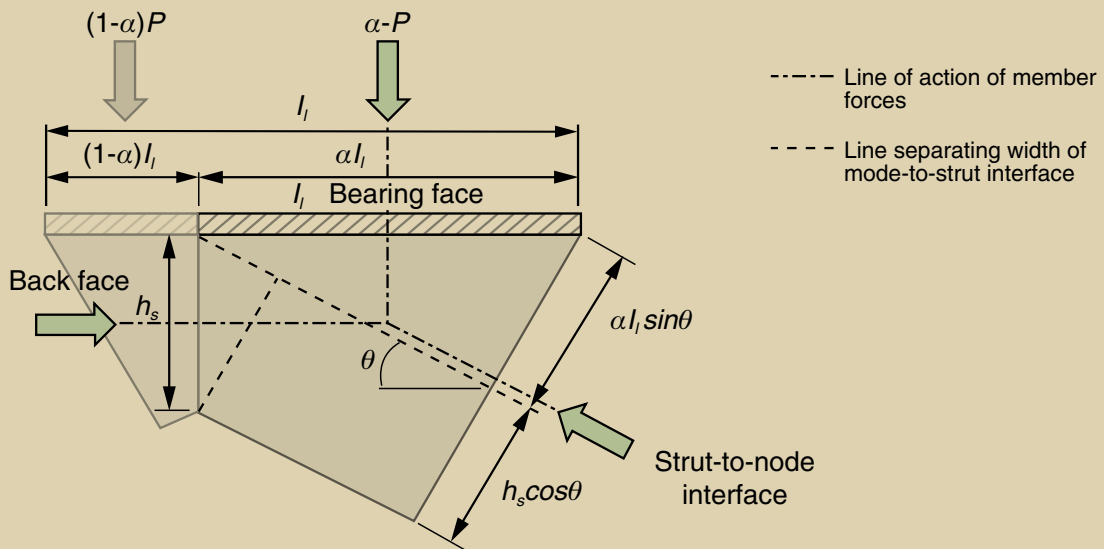
The bearing plate length of a CCT node l_s is determined based on the size of the bearing plate. The height of the back face of a CCT node h_a is taken as twice the distance from the near face of the beam to the centroid of the tension reinforcement.

Deep-beam database

In order to evaluate deep-beam shear provisions, a database containing 868 deep-beam shear tests ($a/d \leq 2.5$) was collected from previous literature. In addition to these 868 tests, Birrcher et al. conducted 37 additional tests.⁸ The database containing all 905 tests is subsequently referred to as the collection database.

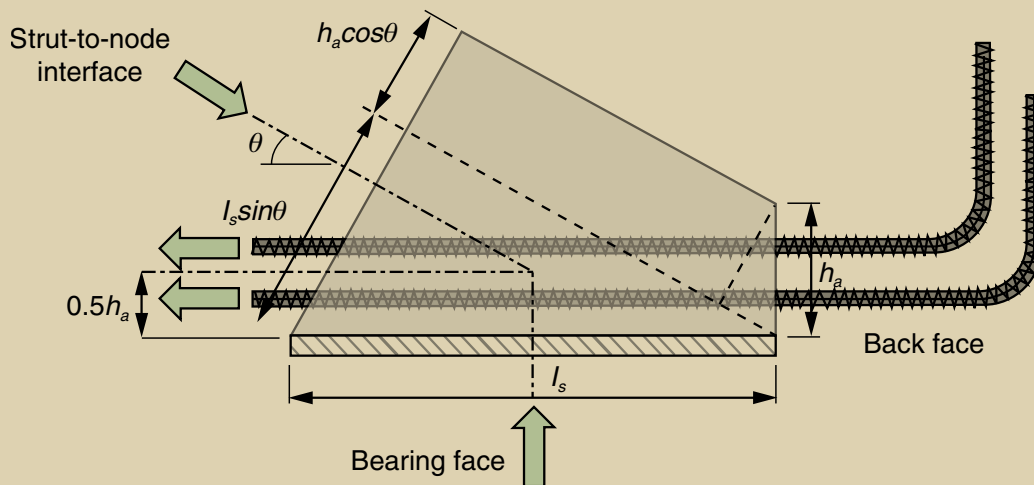
The collection database was filtered in two stages. In the first stage, test results were removed due to a lack of adequate details necessary to perform a strut-and-tie analysis. The resulting database is referred to as the filtered database. In the second stage, additional test results were removed including specimens that were considered less representative of members typically designed in practice. The resulting database is referred to as the evaluation database. **Table 1** provides an overview of the number of specimens that were removed from the database in each stage. Birrcher et al.⁸ provides further explanation of the removal of these test results and a list of the references used to compile the collection database.

The authors' objective is to only consider those beams that better represent actual deep beams designed in practice. **Figure 6** illustrates characteristics of the specimens in the evaluation database.



α = a portion of the applied load that is resisted by near support

CCC node



CCT node

Figure 5. This diagram details the node geometry of a CCC node and CCT node. Note: CCC = node framed by three or more intersecting struts; CCT = node framed by two or more intersecting struts and a tie; h_a = height of the back face of a CCT node; h_s = height of the back face of a CCC node; l_i = length of the bearing plate of a CCC node; l_s = length of the bearing plate of a CCT node; P = axial load; α = portion of the applied load that is resisted by the near support; θ = angle of the strut measured from the horizontal axis.

Evaluation of current design provisions

A total of 179 test results in the evaluation database were used to evaluate the strut-and-tie design provisions in AASHTO LRFD specifications, ACI 318-08, and *fib* struc-

tural concrete. The reported experimental capacity was compared with the strength calculated using the single-panel STM in Fig. 4 with each set of provisions. Based on the nodal geometries given in the model, the following seven stress checks were conducted for all of the beams in the database: back faces of CCC and CCT nodes, bearing faces of CCC and CCT nodes, node-to-strut interfaces at

Table 1. Filtering of the deep-beam database

Collection database		905 tests
Stage 1 filtering	Incomplete plate size information	- 284 tests
	Subjected to uniform loading	- 7 tests
	Stub column failure	- 3 tests
	$f'_c < 2000$ psi	- 4 tests
Filtered database		606 tests
Stage 2 filtering	$b_w < 4.5$ in.	- 222 tests
	$b_w d < 100$ in. ²	- 73 tests
	$d < 12$ in.	- 13 tests
	$\sum \rho_1 < 0.001$	- 120 tests
Evaluation database		179 tests

Note: b_w = width of beam web; d = distance from extreme compression fiber to centroid of longitudinal tension reinforcement; f'_c = specified compressive strength of concrete; $\sum \rho_1$ = summation of transverse reinforcement (defined in ACI 318-08).

Table 2. Summary of stress checks used to evaluate deep beams

Element	Design check	Design provisions	Allowable stress
CCC node	Bearing	AASHTO LRFD specifications	$0.85f'_c$
		ACI 318-08	$0.85f'_c$
		<i>fib</i> structural concrete	$0.85(1 - f'_c/40\text{ksi})f'_c$
	Back face	AASHTO LRFD specifications	$0.8f'_c$
		ACI 318-08	$0.85f'_c$
		<i>fib</i> structural concrete	$0.85(1 - f'_c/40\text{ksi})f'_c$
	Node-to-strut interface	AASHTO LRFD specifications	$0.85f'_c$
		ACI 318-08	$0.85(0.75)f'_c = 0.64f'_c$
		<i>fib</i> structural concrete	$0.85(1 - f'_c/40\text{ksi})f'_c$
CCT node	Bearing	AASHTO LRFD specifications	$0.75f'_c$
		ACI 318-08	$0.85(0.80)f'_c = 0.68f'_c$
		<i>fib</i> structural concrete	$0.70(1 - f'_c/40\text{ksi})f'_c$
	Back face	AASHTO LRFD specifications	$0.75f'_c$
		ACI 318-08	$0.85(0.80)f'_c = 0.68f'_c$
		<i>fib</i> structural concrete	n.a.
	Node-to-strut interface	AASHTO LRFD specifications	$f'_c/(0.8 + 170\varepsilon_1) \leq 0.85f'_c$
		ACI 318-08	$0.85(0.75)f'_c = 0.64f'_c$
		<i>fib</i> structural concrete	$0.70(1 - f'_c/40\text{ksi})f'_c$
Tie	Tie	All	f_y

Note: CCC = node framed by three or more intersecting struts; CCT = node framed by two or more intersecting struts and a tie; f'_c = specified compressive strength of concrete; f_y = specified yield strength of tensile reinforcement; n.a. = not applicable; ε_1 = principle tensile strain in cracked concrete.

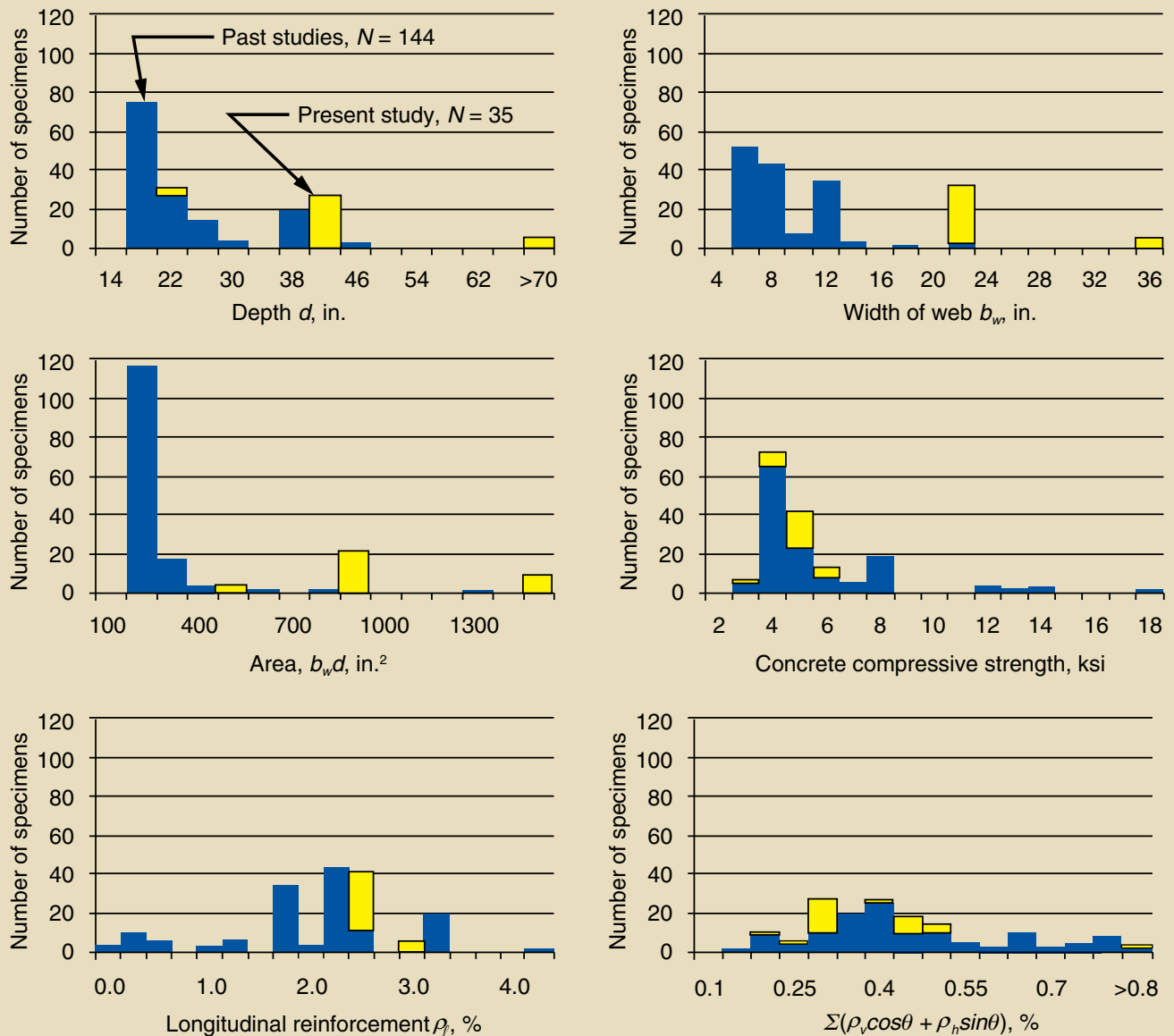


Figure 6. These histograms summarize the characteristics of the test specimens contained in the evaluation database. Note: b_w = width of beam web; d = distance from extreme compression fiber to centroid of longitudinal tension reinforcement; N = number of test specimens that are evaluated; θ = angle of the strut measured from the horizontal axis; ρ_l = ratio of horizontal shear reinforcement area to gross area of vertical section; ρ_v = ratio of horizontal shear reinforcement area to gross area of horizontal section. 1 in. = 25.4 mm; 1 ksi = 6.895 MPa.

the CCC and CCT nodes, and stress in the tie reinforcement. The governing design check determined the calculated capacity of the specimen.

The stress checks account for the possible failure modes of a deep beam with two detailing exceptions. Proper anchorage of the tie must be provided to ensure that the tie reaches its design force. Similarly, minimum web reinforcement is required to provide a deep beam with sufficient deformation capacity to prevent premature splitting of the strut. All of the specimens in the database contained adequate anchorage and a minimum amount of web reinforcement to avoid these premature failure modes.

Table 2 lists the allowable stress used from each set of STM provisions. Additional information regarding each allowable stress can be found in the respective design specification. The ratio of experimental to calculated capacity was determined for the beams in the evaluation database using the aforementioned design provisions and strut-and-tie model. **Figure 7** presents a histogram of the findings.

When the experimentally determined capacity is greater than or equal to the calculated capacity (experimental/calculated > 1), the estimation of strength is a conservative prediction. Upon examination of the data in Fig. 7, it can be concluded that all three procedures provide adequately conservative estimates of strength. In all cases, less than

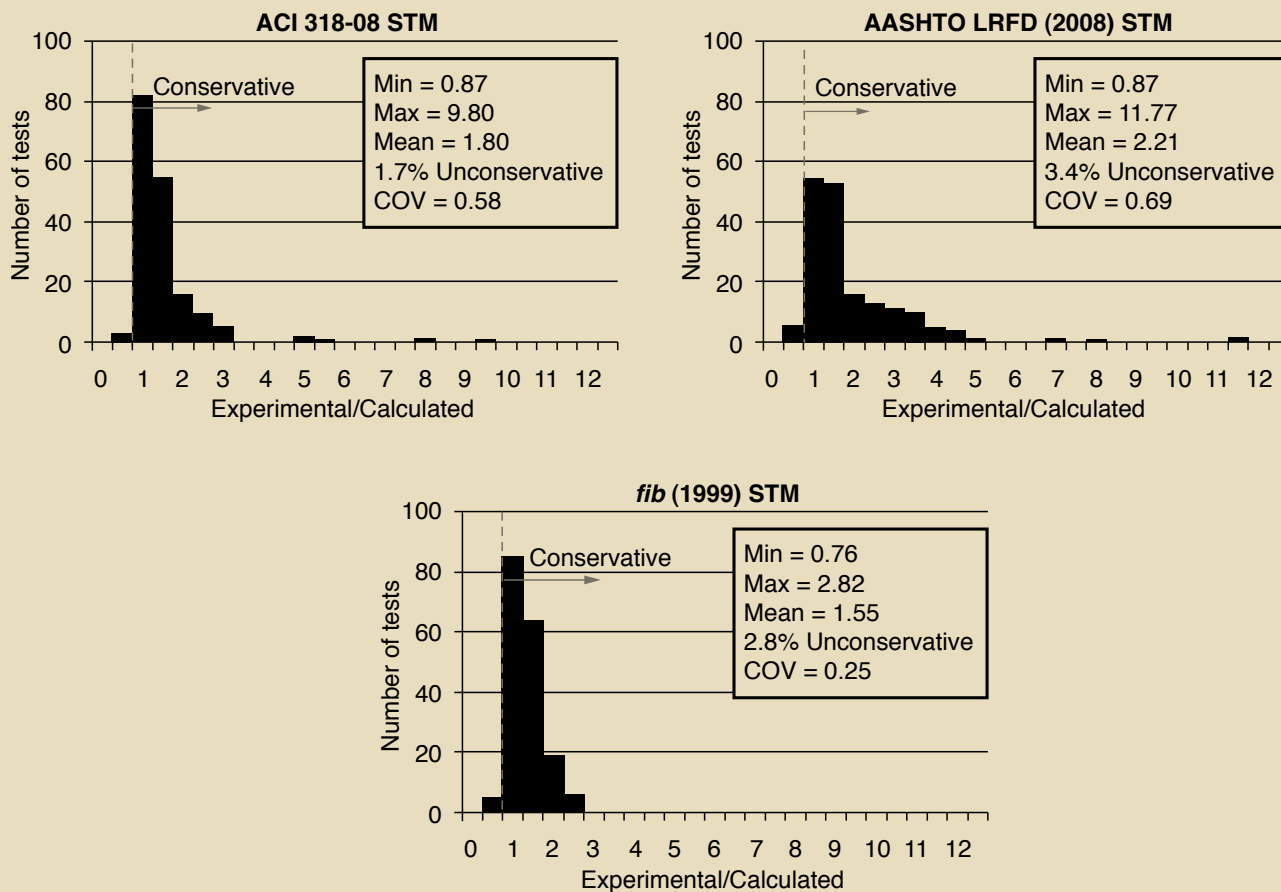


Figure 7. These histograms summarize the ratio of the experimental capacity over the STM estimation for all of the beams in the evaluation database ($N = 179$). Note: COV = coefficient of variation; N = number of test specimens that are evaluated; STM = strut-and-tie model.

5% of the test data were unconservatively estimated. However, there was a considerable difference in the accuracy of each set of STM provisions as measured by the coefficient of variation (COV) and the mean ratio of experimental to calculated value. The implication of a high COV is an unnecessarily conservative estimate of strength. For example, the mean experimental-to-calculated ratio for the AASHTO LRFD specifications (2.21) is 30% higher than it is for the *fib* structural concrete provisions (1.55). Therefore, on average, a beam designed according to AASHTO LRFD specifications would have 30% less design capacity than the same beam if it were designed according to *fib* structural concrete. In addition, two of the beams in the database carried an ultimate load almost 12 times greater than the AASHTO LRFD specifications design capacity.

With a COV of 0.69 and a mean experimental-to-calculated value of 2.21, the STM procedure in the AASHTO LRFD specifications was the least accurate design method. The reason can be attributed to the derivation of the method; it was likely derived using hydrostatic rather than nonhydrostatic nodes. According to the AASHTO LRFD specifications, the allowable stress at the CCT node-to-strut interface (Table 2) decreases as the *ald* increases. If this decrease in allowable

stress is taken in combination with an increasing hydrostatic node size (Fig. 3), then the accuracy of the method is improved. On the contrary, if a decrease in allowable stress is taken in combination with a relatively unchanged nonhydrostatic node size, then the estimation of strength is more conservative. As noted previously, the use of nonhydrostatic nodes is more appropriate for design.

The *fib* structural concrete method is considerably more accurate than the other two methods. This method has a COV of 0.25 compared with 0.58 for ACI 318-08 and 0.69 for AASHTO LRFD specifications. The difference in accuracy can be attributed to the following:

- Triaxial confinement: *fib* structural concrete explicitly permits the allowable stress at all faces of a nodal zone to be increased when concrete surrounding the loaded area provides triaxial confinement.
- Back face of CCT node: *fib* structural concrete does not consider bonding stresses at the back face of a CCT node to be critical if reinforcing bars are anchored properly.

- Decrease in efficiency factors with an increase in concrete strength: As the compressive strength of concrete increases, its efficiency decreases. As a result, its capacity increases at a diminishing rate.

The authors' goal is to suggest improvements to the ACI 318-08 and AASHTO LRFD specifications STM provisions. Based on the data in Fig. 7, the *fib* structural concrete procedure is the most accurate. According to MacGregor,⁹ an STM design procedure should satisfy four criteria:

- simplicity in application
- compatibility with tests of D regions
- compatibility with other sections of the code
- compatibility with other codes or design recommendations

With these considerations in mind, the authors propose a strut-and-tie design method that is largely based on the provisions in *fib* structural concrete but is compatible with other articles of ACI 318-08 and AASHTO LRFD specifications.

Proposed strut-and-tie design method

The following method is recommended for STM design.

Equation (2) calculates the nominal strength of a nodal zone F_n .

$$F_n = f_{ce} A_{nz} \quad \text{Eq. (2)}$$

where

f_{ce} = effective compressive strength of concrete in nodal zone

A_{nz} = cross-sectional area of the face of the nodal zone

Equation (3) determines the effective compressive strength on the face of a nodal zone f_{ce} .

$$f_{ce} = mv f'_c \quad \text{Eq. (3)}$$

where

$m = \sqrt{\frac{A_2}{A_1}} \leq 2$ triaxial confinement modification factor, as defined in ACI 318-08 and AASHTO LRFD specifications

A_2 = area of the lower base of the largest frustum of a pyramid, cone, or tapered wedge contained wholly within the support and having for its upper base the

loaded area and having side slopes of 1 vertical to 2 horizontal

A_1 = loaded area

ν = concrete efficiency factor

= 0.85 for bearing and back face of CCC nodes

= 0.70 for bearing and back face of CCT nodes

$0.45 \leq \left(0.85 - \frac{f'_c}{20}\right) \leq 0.65$ for CCC and CCT node-to-strut interfaces with crack control reinforcement

= 0.45 for CCC and CCT node-to-strut interfaces without crack-control reinforcement

f'_c = specified compressive strength of concrete

Commentary on the proposed method

The triaxial confinement modification factor m is recognized in bearing calculations in AASHTO LRFD specifications and ACI 318-08 but not in their respective STM provisions. The strength and ductility of concrete are higher under triaxial compression than under uniaxial compression.¹⁰ To confirm that triaxial confinement was applicable to deep-beam tests, the authors tested several specimens in the current study.⁸ The dimensions of the bearing plates were the primary variable. The test results support the benefits of triaxial confinement of surrounding concrete for all faces of nodal regions. Based on experimental data and while maintaining compatibility with bearing calculations in AASHTO LRFD specifications and ACI 318-08, the same modification factor is recommended in the proposed STM provisions.

The concrete efficiency factor ν is similar to that in AASHTO LRFD specifications and ACI 318-08 for the bearing face at CCC and CCT nodes and for the back face of CCC nodes. However, for the back face of CCT nodes, bond stresses from an adequately developed tension tie (**Fig. 8**) are not applied to the back face of the node. Based on the experimental results of this testing program,⁸ recommendations of *fib* structural concrete, recommendations of past researchers,^{11,12} and an analysis of the database,⁸ it was determined that it is unnecessary to apply the bonding stresses from a developed bar to the back face of a CCT node. Therefore, only directly applied stresses, such as those due to bearing of a plate or to an external indeterminacy (Fig. 8), are applied to the back face of CCT nodes and checked with the 0.70 efficiency factor.

In the proposed STM provisions (Eq. [3]), the efficiency factor at the node-to-strut interface varies with the compressive strength of concrete and has a minimum and

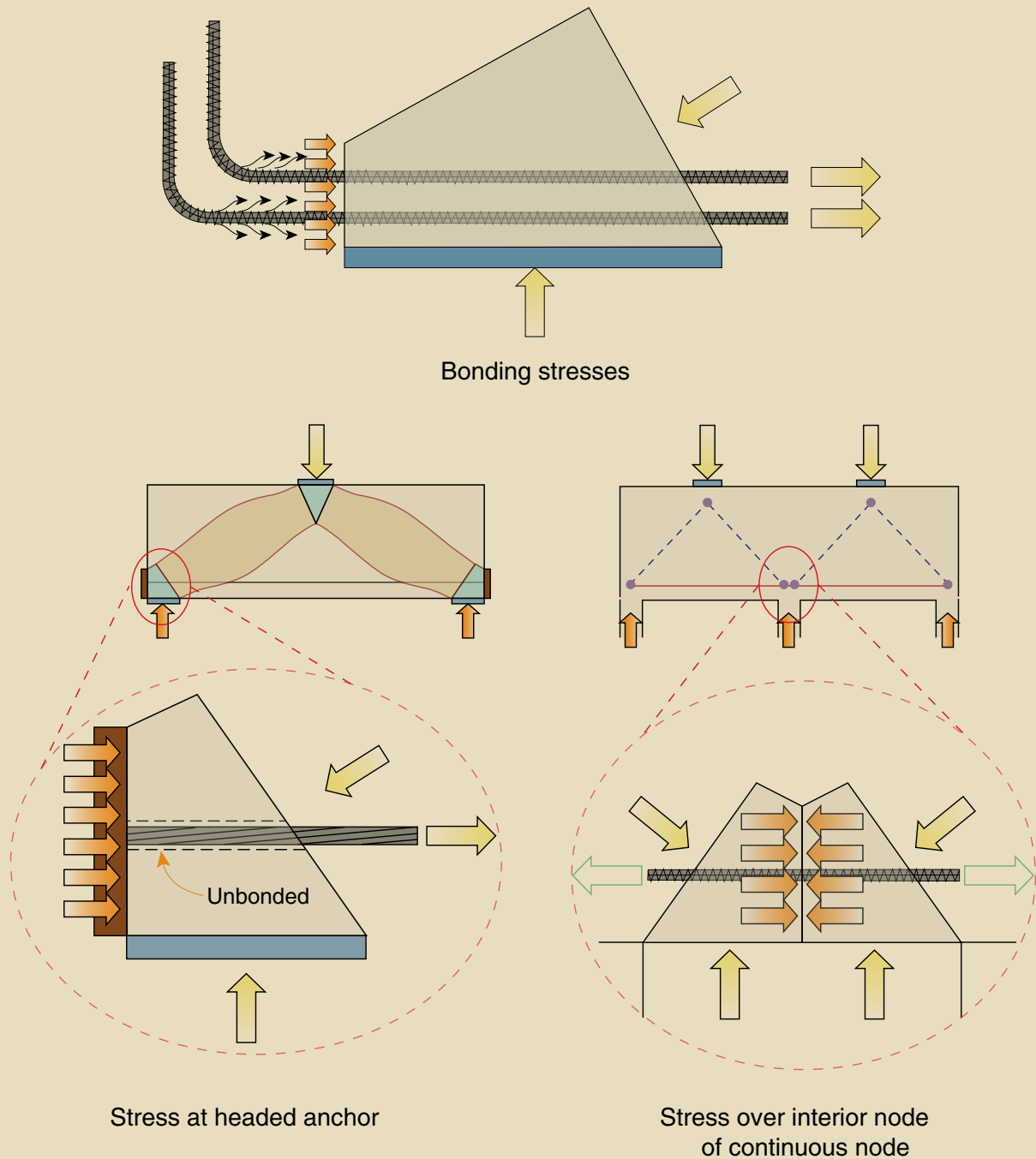


Figure 8. This figure illustrates the three different stress conditions that can occur at the back face of a CCT node. CCT = node framed by two or more intersecting struts and a tie.

maximum limit of 0.45 and 0.65, respectively. Premature strut splitting is avoided by providing orthogonal grids of web reinforcement or by limiting the efficiency factor at the node-to-strut interface to 0.45.

No concrete stress checks are required in Eq. (3) for CTT nodes or other similarly smeared nodal regions. Smeared nodes refer to those regions that are not bounded by a

bearing plate. Forces from compressive struts spread—and smear—and are equilibrated by multiple stirrups or ties. According to Schlaich et al.,¹³ the geometry of smeared nodes is not discrete, and therefore, checking stress limits is unnecessary. Tension reinforcement in CTT nodes near reentrant corners or voids should be well distributed in order to reduce high stress concentrations,⁴ and ties in CTT nodes must be adequately developed or anchored.

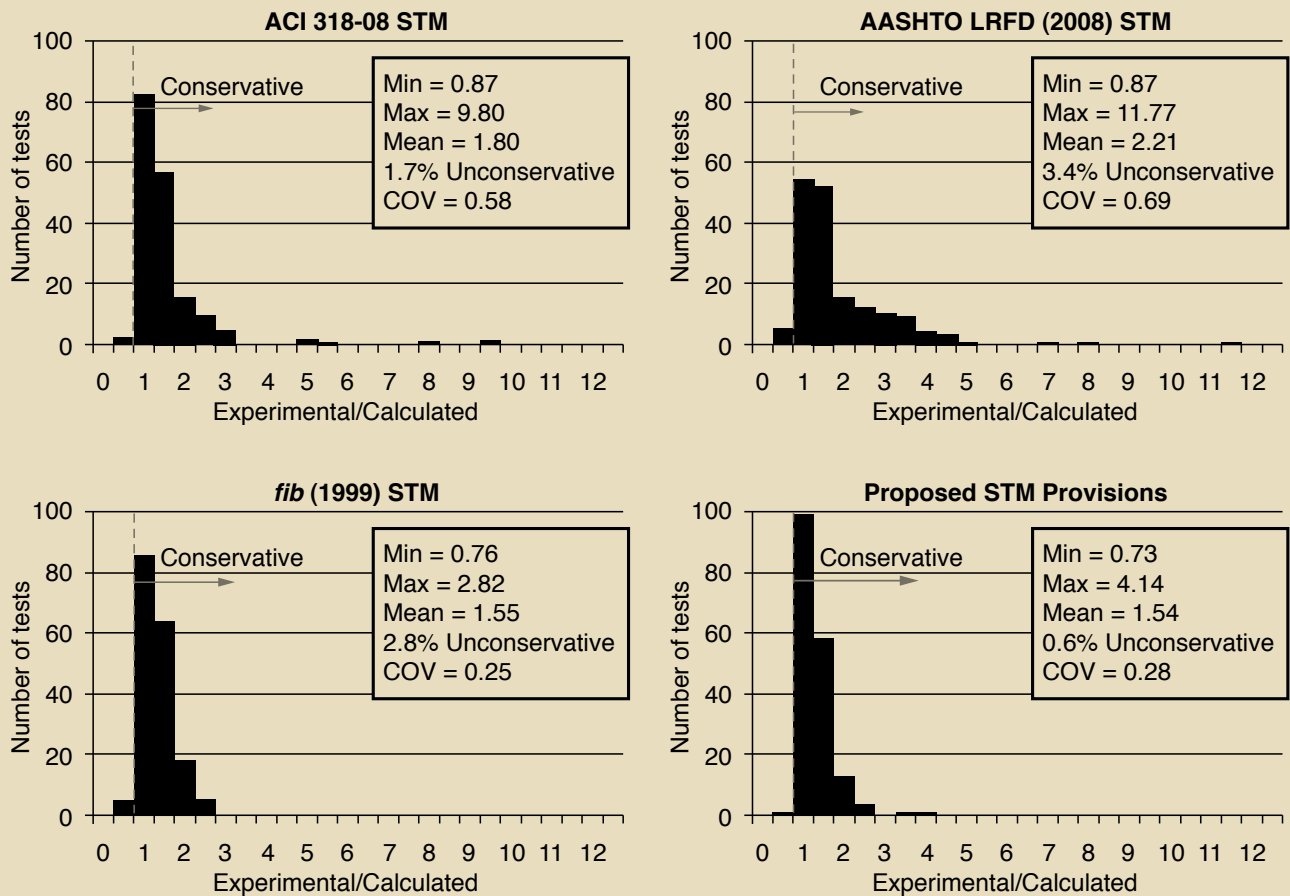


Figure 9. These histograms summarize the ratio of the experimental capacity over the STM estimation for all of the beams in the evaluation database. The design provisions presented in Fig. 7 are compared with the new method proposed in this paper ($N = 179$). Note: COV = coefficient of variation; N = number of test specimens that are evaluated; STM = strut-and-tie model.

The recommendations outlined by *fib* structural concrete were used to formulate a new STM design procedure. The following attributes of the proposed STM design procedure are consistent with the *fib* structural concrete provisions:

- Disregard the stress check at the back face of the CCT node when the applied force is the resultant of bonding stresses from a sufficiently anchored tie.
- Increase the allowable stress in triaxially confined nodal regions.
- At the CCC and CCT strut-to-node interface, the efficiency of concrete decreases as the compressive strength increases.

The following attributes of the proposed STM provisions are consistent with the ACI 318-08 and AASHTO LRFD specifications provisions:

- A triaxial confinement modification factor is used to account for the increase in nodal capacity due to triax-

ial confinement. The modification factor is expressed the same as for bearing capacity.

- In accordance with ACI 318-08, the efficiency of the CCC and CCT node-to-strut interfaces is identical.
- At the bearing and back faces of the CCC node, the efficiency of concrete is a constant value of 0.85.
- At the bearing face of the CCT node, the efficiency of concrete is a constant value of 0.70.

Assessment of the proposed strut-and-tie design method

Figure 9 presents an assessment of the proposed method. The ratio of experimental to calculated shear capacity is determined for the beams in the evaluation database and presented in the same manner as previously shown (Fig. 7). The proposed STM procedure is a significant improvement over the current ACI 318-08 and AASHTO LRFD specifications procedures.

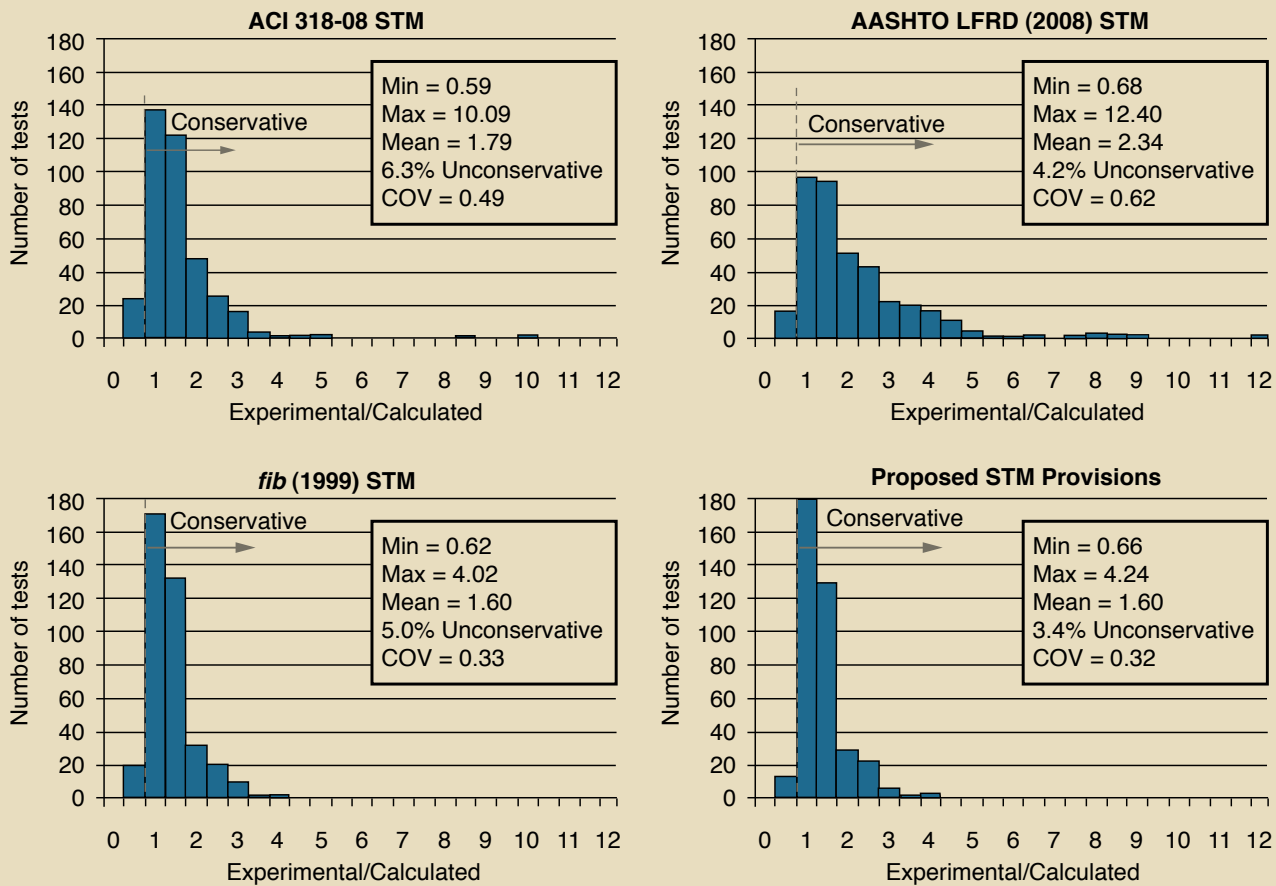


Figure 10. These histograms summarize the ratio of the experimental capacity over the STM estimation for all of the beams in the filtered database with $\rho_t > 0.1\%$ ($N = 382$). Note: COV = coefficient of variation; N = number of test specimens that are evaluated; STM = strut-and-tie model; ρ_t = ratio of the shear reinforcement perpendicular to the plane of the strut.

The specimens in the evaluation database were selected because they more accurately represent beams designed in practice in terms of both their size and reinforcement details. The authors determined the criteria used to select these test specimens (Table 1). It is also of interest to evaluate the performance of the proposed provisions for a data set other than that used to calibrate the proposed procedure. Accordingly, the proposed STM provisions are compared for all of the beams in the filtered database that contain a minimum amount of transverse reinforcement (Fig. 10).

The tests evaluated in Fig. 10 constitute every deep-beam shear test that could be found in the literature if the test contained adequate bearing-plate information and a minimal amount of transverse reinforcement. Although many of the beams in the filtered database were not used to calibrate the authors' recommendations, the proposed STM procedure is a significant improvement over the ACI 318-08 and AASHTO LRFD specifications provisions.

Conclusion

A new STM design procedure was developed for the design of deep beams while maintaining consistency with current provisions and established principles. Based on the results of this study, the authors strongly believe that the proposed STM method is valid for other types of structures.

In developing an STM procedure, it was necessary to explicitly define the truss geometries. This step cannot be overemphasized because the performance of an STM methodology and its efficiency factors are intrinsically linked to the geometry of the nodal regions. Thus, the proposed STM provisions are based on an explicitly defined single-panel truss model with nonhydrostatic nodes. This single-panel model may be used as a basis for determining the configuration of forces in most deep-beam regions.

Another important aspect of the new STM design methodology is that it was comprehensively derived based on all of the stress checks that constitute an STM design. Stress checks at all six nodal faces (three faces at CCC and three faces at CCT nodes) and in the longitudinal tie were

performed for all of the beams in the evaluation database. The splitting of the strut was indirectly accounted for by only considering those beams that contained a minimum amount of transverse reinforcement. Thus, the newly proposed design procedure considers every facet of an STM design. The newly proposed STM procedure is simpler and more accurate than the ACI 318-08 and AASHTO LRFD specifications STM design provisions, but is just as safe. The procedure is based on established principles of strut-and-tie design, on tests of D regions, and on the procedures in ACI 318-08, AASHTO LRFD specifications, and *fib* structural concrete STM provisions. Finally, the procedure is practical and has been derived in a comprehensive and transparent manner.

Acknowledgments

The authors are sincerely grateful to the Texas Department of Transportation (TxDOT) for providing the funds to conduct this research study. The recommendations of project director Dean Van Landuyt (Bridge Division) and other members of TxDOT, including John Vogel (Houston District) and David Hohmann (Bridge Division), are deeply appreciated.

The authors would like to thank Matt Huizinga for his technical contributions and assistance with the experimental portion of the project. In addition, the recommendations of James Jirsa, Sharon Wood, and John Breen improved the quality of this research and are greatly valued.

References

1. American Concrete Institute (ACI) Committee 318. 2008. *Building Code Requirements for Reinforced Concrete (ACI 318-08) and Commentary (ACI 318R-08)*. Farmington Hills, MI: ACI.
2. American Association of State Highway and Transportation Officials (AASHTO). 2007. *AASHTO LRFD Bridge Design Specifications*. 4th ed. Washington, DC: AASHTO.
3. AASHTO. 2008. *AASHTO LRFD Bridge Design Specifications, 4th Edition—2008 Interim Revisions*. Washington, DC: AASHTO.
4. *fib*. 1999. *Structural Concrete—Textbook on Behaviour, Design, and Performance*. V. 3. Lausanne, Switzerland: *fib*.
5. MacGregor, J. G. 1997. *Reinforced Concrete, Mechanics and Design*. 3rd ed. Upper Saddle River, NJ: Prentice Hall.
6. Collins, M. P., and D. Mitchell. 1997. *Prestressed Concrete Structures*. Toronto, ON, and Montreal, QC, Canada: Response Publications.
7. Kani, M. W., M. W. Huggins, and R. R. Wittkopp, eds. 1979. *Kani on Shear in Reinforced Concrete*. Toronto, ON, Canada: University of Toronto Press.
8. Birrcher, D. B., R. G. Tuchscherer, M. R. Huizinga, O. Bayrak, S. L. Wood, and J. O. Jirsa. 2009. *Strength and Serviceability Design of Reinforced Concrete Deep Beams*. Report no. 0-5253-1. Austin, TX: Center for Transportation Research, University of Texas at Austin.
9. MacGregor, J. G. 2002. Derivation of Strut and Tie Models for the 2002 ACI Code. In *ACI SP-208 Examples for the Design of Structural Concrete with Strut-and-Tie Models*. Farmington Hills, MI: ACI.
10. MacGregor, J. G., and J. K. Wight. 2005. *Reinforced Concrete, Mechanics and Design*. 4th ed. Upper Saddle River, NJ: Pearson Prentice Hall.
11. Thompson, M. K., M. J. Young, J. O. Jirsa, J. E. Breen, and R. E. Klingner. 2003. *Anchorage of Headed Reinforcement in CCT Nodes*. Research report 1855-2. Austin, TX: Center for Transportation Research, University of Texas at Austin.
12. Brown, M. D., C. L. Sankovich, O. Bayrak, J. O. Jirsa, J. E. Breen, and S. L. Wood. 2006. *Design for Shear in Reinforced Concrete Using Strut-and-Tie Models*. Report No. 0-4371-2. Austin, TX: Center for Transportation Research, University of Texas at Austin.
13. Schlaich, J., K. Schäfer, and M. Jennewein. 1987. Toward a Consistent Design of Structural Concrete. *PCI Journal*, V. 32, No. 3 (May–June): pp. 74–150.

Notation

a = shear span

a/d = shear span-to-depth ratio measured from center of span to center of support

A_1 = loaded area

A_2 = area of the lower base of the largest frustum of a pyramid, cone, or tapered wedge contained wholly within the support and having for its upper base the loaded area and having side slopes of 1 vertical to 2 horizontal

A_{nz} = cross-sectional area of the face of a nodal zone

A_s	= area of tension reinforcement		crete area of vertical section
A'_s	= area of compression reinforcement	ρ_l	= longitudinal reinforcement
b_w	= width of beam web	ρ_v	= ratio of vertical shear reinforcement to gross concrete area of horizontal section
c	= distance from extreme compression fiber to neutral axis	ρ_{\perp}	= ratio of the shear reinforcement perpendicular to the gross concrete area in the plane of the strut
d	= depth of member taken as the distance from extreme compression fiber to centroid of longitudinal tension reinforcement	θ	= angle of strut measured from the horizontal axis
f'_c	= specified compressive strength of concrete	ν	= efficiency factor, concrete effectiveness factor
f_{ce}	= effective compressive strength of concrete in nodal zone		
f_s	= stress in tension reinforcement		
f'_s	= stress in compression reinforcement		
f_y	= specified yield strength of tensile reinforcement		
F_n	= nominal strength of a nodal zone		
h	= overall height of member		
h_a	= height of the back face of a CCT node taken as twice the distance from extreme tension fiber to centroid of longitudinal tension reinforcement		
h_s	= height of the back face of a CCC node taken as the height of the equivalent stress block in the flexural compression zone		
l_l	= length of the bearing plate at the CCC node		
l_n	= span (from McGregor ⁵)		
l_s	= length of the bearing plate at the CCT node		
m	= triaxial confinement modification factor =		
	$\sqrt{\frac{A_2}{A_1}} \leq 2$		
P	= axial load		
α	= proportion of applied load that is resisted by the near support		
β_1	= factor for proportioning the depth of the equivalent stress block in the flexural compression region		
ϵ_1	= principal tensile strain in cracked concrete		
ρ_h	= ratio of horizontal shear reinforcement to gross con-		

About the authors



Robin Tuchscherer, P.E., PhD, is a project engineer at Datum Engineers Inc. in Austin, Tex.



David Birrcher, PhD, is a bridge designer at International Bridge Technologies Inc. in San Diego, Calif.



Oguzhan Bayrak, P.E., PhD, is an associate professor of civil, architectural, and environmental engineering at the University of Texas at Austin. He serves as director of the Phil M. Ferguson Structural Engineering Laboratory

and holds the Charles Elmer Rowe Fellowship in the Cockrell School of Engineering.

Synopsis

The overall objective of the research project summarized in this paper was to develop simple and safe design guidelines for deep beams. To accomplish the research objective and related tasks, a database of 868 deep-beam tests was assembled from previous research. In addition, 37 beams were fabricated and tested with the following cross-sectional dimensions: 36 in. × 48 in. (910 mm × 1220 mm), 21 in. × 75 in. (530 mm × 1910 mm), 21 in. × 42 in. (530 mm ×

1070 mm), and 21 in. × 23 in. (530 mm × 580 mm). These tests represent some of the largest deep-beam shear tests ever conducted. Based on an analysis of the database and the experimental program, the deep-beam shear provisions in *Building Code Requirements for Reinforced Concrete (ACI 318-08)* and *AASHTO LRFD Bridge Design Specifications* were found to be overly conservative. Thus, a new and simple strut-and-tie modeling (STM) procedure was proposed for the strength design of deep-beam regions. The procedure is largely based on the *fib* structural concrete design provisions. It is more accurate than the STM design method in ACI 318-08 and AASHTO LRFD specifications but just as conservative. With the use of the proposed provisions, the design of deep beams is more efficient and reliable. As a result, implementation of the new design provisions into ACI 318-08 and AASHTO LRFD specifications is recommended.

Keywords

Deep beam, efficiency factors, shear, STM, strut-and-tie modeling, triaxial confinement.

Review policy

This paper was reviewed in accordance with the Precast/Prestressed Concrete Institute's peer-review process.

Reader comments

Please address any reader comments to journal@pci.org or Precast/Prestressed Concrete Institute, c/o *PCI Journal*, 200 W. Adams St., Suite 2100, Chicago, IL 60606. 